

## Photochemical and Photophysical Deactivation of 2,4,6-Triaryl-1,3,5-triazines

Frank Elbe,<sup>†</sup> Juergen Keck,<sup>†</sup> Anja P. Fluegge,<sup>†</sup> Horst E. A. Kramer,<sup>\*,†</sup> Peter Fischer,<sup>\*,‡</sup> Pascal Hayoz,<sup>§</sup> David Leppard,<sup>§</sup> Gerhard Rytz,<sup>§,¶</sup> Wolfgang Kaim,<sup>||</sup> and Michael Ketterle<sup>||</sup>

*Institut für Physikalische Chemie, Institut für Organische Chemie, and Institut für Anorganische Chemie, Universität Stuttgart, Pfaffenwaldring 55, D-70569 Stuttgart, Germany, and Ciba Specialty Chemicals, Inc., Additives Division, Rosental R 1059, CH-4002 Basel, Switzerland*

Received: January 6, 2000; In Final Form: April 14, 2000

Both UV absorption and fluorescence maxima of 2-(2-methoxyaryl)-1,3,5-triazines show a marked bathochromic shift with increasing proton concentration. Well-defined isosbestic points establish an equilibrium between protonated and nonprotonated species for the ground state. <sup>1</sup>H and <sup>13</sup>C NMR data unequivocally prove a rapid prototropic equilibrium ( $> 10^2$ /s) between tautomers protonated at N-1, N-3, and N-5, respectively. The NMR data also show a substantial increase in charge transfer, upon protonation, from the phenyl, and even more from the alkoxy-substituted aryl rings into the triazine system already for the ground state. At higher proton concentrations, the twisted intramolecular charge transfer (TICT) fluorescence of the nonprotonated (2-methoxyaryl) triazines is gradually replaced by the much weaker fluorescence of the protonated species, which is shifted to still longer wavelengths. Because the electron-accepting capacity of triazines is enhanced in the excited state, their  $pK_a$  values increase, upon photoexcitation, by 6.8–9 units; thence, the excited-state energy level of the protonated form ( $S_1'$ ) is calculated to be lower by 37–51 kJ/mol than that of the respective nonprotonated species ( $S_1$ ). Protonation thus leads to static quenching of the fluorescence. Halide ions, in contrast, can act as external electron donors toward triazines only in their highly electron-affine excited state, and so effect merely dynamic fluorescence quenching, with a corresponding reduction in fluorescence quantum yield, for the (2-methoxyaryl) triazines. Photochemical stabilization by protonation, therefore, is more efficient than by electron transfer. For all systems investigated, the excited-state electron transfer is exergonic and hence may be considered as diffusion-controlled, in accordance with the Rehm–Weller equation.

## 1. Introduction

Compounds with an intramolecular hydrogen bridge (IMHB), such as methyl salicylates, *o*-hydroxybenzophenones, 2-(2-hydroxyaryl)benzotriazoles, and 2-(2-hydroxyaryl)-1,3,5-triazines are widely used for the photostabilization of polymers.<sup>1–19</sup> They absorb harmful UV radiation and transform it, via a very efficient excited-state intramolecular proton transfer (ESIPT) within the IMHB, into vibrational energy.<sup>4–34</sup> Electronic relaxation and subsequent proton back-transfer in the ground state complete a four-level sequence that constitutes a true intramolecular Förster cycle. The IMHB can be broken, though, by basic agents or, especially in the benzotriazoles, certain polar solvents, for example, dimethyl sulfoxide.<sup>6,9,11,19,33,35–37</sup> Without an intact IMHB, both the photostability of the UV absorber and its effectiveness as a polymer-protecting additive appear critically reduced.

The IMHB of 2-(2-hydroxyaryl)-1,3,5-triazines has been shown to be exceptionally strong and stable, and thence is far less susceptible to external influences than the IMHB of

benzotriazoles.<sup>38</sup> Definite proof has accumulated, however, that in polar matrixes (and many polymer coatings constitute a rather polar environment) even the IMHB of such (2-hydroxyaryl) triazines can be broken.<sup>39</sup> It seemed desirable, therefore, to conceive UV stabilizers which, rather than depending on an IMHB for their efficiency, would offer alternative deactivation pathways. New fields thus might be opened up for the application of UV stabilizers of this type, which so far are closed because of the sensitivity of the intramolecular hydrogen bond.

Intramolecular electron transfer, with a four-level cycle analogous to the proton-transfer cycle, could likewise accelerate radiationless deactivation and thus provide for the essential photochemical stability of UV absorber molecules which lack the Achilles heel of an IMHB. We now report on two different approaches to realize this objective. For one, we studied the effect of protonation on a number of *O*-methyl derivatives of established 2-(2-hydroxyaryl)-1,3,5-triazine UV absorbers which have the bridging OH function replaced by an alkoxy moiety. These compounds, which as such are but poor stabilizers, exhibit a moderately intense Twisted Intramolecular Charge Transfer (TICT) fluorescence. Protonation, by raising the electron acceptor capacity of the triazine core, should enhance intramolecular electron transfer and thence favor radiationless deactivation. Second, we investigated whether addition of external electron donors to such (methoxyaryl) triazines could likewise provide for photoinduced electron transfer.

\* To whom correspondence should be addressed. Fax: 0049-711-685-4495.

<sup>†</sup> Institut für Physikalische Chemie.

<sup>‡</sup> Institut für Organische Chemie.

<sup>§</sup> Ciba Specialty Chemicals, Inc.

<sup>||</sup> Institut für Anorganische Chemie.

<sup>¶</sup> Present address: Vigier Cément, CH-2603 Péry, Switzerland.

## 2. Experimental Section

**2.1. Materials.** *Triazine, Pyrimidine, and Pyridine Derivatives.* All compounds, listed below with both their systematic name and symbol designation, were synthesized in the laboratories of Ciba Specialty Chemicals, Inc., Marly, Switzerland, and purified by recrystallization from toluene (for molecular structures, see Chart 1.)

2,4,6-triphenyl-1,3,5-triazine	(TPT)
2-(2-methoxyphenyl)-4,6-diphenyl-1,3,5-triazine	(2-MOTT-2)
2-(4-methoxyphenyl)-4,6-diphenyl-1,3,5-triazine	(2-MOTT-4)
2,4-bis(4-methoxyphenyl)-6-phenyl-1,3,5-triazine	(2,4-MOTT-4)
2,4,6-tris(4-methoxyphenyl)-1,3,5-triazine	(2,4,6-MOTT-4)
2-(2,4-dimethoxyphenyl)-4,6-diphenyl-1,3,5-triazine	(M-MeO-P)
2,4-diphenyl-6-(4-dodecyloxy-2-methoxyphenyl)-1,3,5-triazine	(D-MeO-P)
2-(2,4-dimethoxyphenyl)-4,6-bis(4-methylphenyl)-1,3,5-triazine	(M-MeO-T)
2-(4-hexoxy-2-methoxyphenyl)-4,6-bis(4-methylphenyl)-1,3,5-triazine	(H-MeO-T)
2-(2,4-dimethoxyphenyl)-4,6-bis(2,4-dimethylphenyl)-1,3,5-triazine	(M-MeO-X)
2,4-bis(2,4-dimethylphenyl)-6-(4-dodecyloxy-2-methoxyphenyl)-1,3,5-triazine	(D-MeO-X)
2-(2-hydroxyphenyl)-4,6-diphenyl-1,3,5-triazine	(2-HTT-2)
2,4-bis(2-hydroxyphenyl)-6-phenyl-1,3,5-triazine	(2,4-HTT-2)
2,4-diphenyl-6-pyrrolidino-1,3,5-triazine	(N2-DTZ)
2,4-diphenyl-6-piperidino-1,3,5-triazine	(N3-DTZ)
2,4-diphenyl-6-morpholino-1,3,5-triazine	(N4-DTZ)
2,4-bis[4-(3-butoxy-2-hydroxypropoxy)-2-hydroxyphenyl]-6-phenyl-1,3-diazine	(BHD)
4-(2,4-dihexoxyphenyl)-2-(4-hexoxy-2-hydroxyphenyl)-6-(4-methoxyphenyl)-1,3-diazine	(HDD)
2,4-bis(4-hexoxy-2-hydroxyphenyl)-6-(4-methoxyphenyl)-1,3-diazine	(HMD)
2-(2-hydroxyphenyl)-4,6-diphenylpyridine	(HDP)

**Solvents.** Acetic anhydride (>99.5%, Fluka), acetonitrile (Uvasol, Merck), perchloric acid (0.1 N solution in glacial acetic acid, Aldrich) were used as supplied. Diethyl ether (Uvasol 1, Merck) was dried with CaCl<sub>2</sub> and distilled over CaH<sub>2</sub>; ethanol (99.9+, Aldrich) was dried and distilled over CaH<sub>2</sub>; 3-methylpentane was washed first with H<sub>2</sub>SO<sub>4</sub>, then with H<sub>2</sub>O/Na<sub>2</sub>CO<sub>3</sub>, dried with CaH<sub>2</sub>, and distilled.

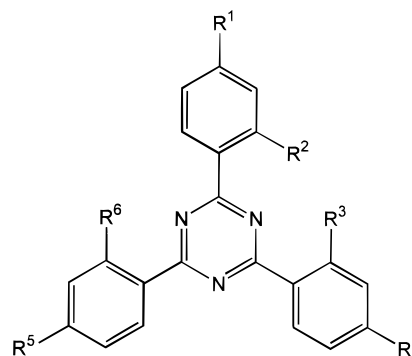
**Salts.** NEt<sub>4</sub>J (>99%, Merck), KSCN (>98%, Fluka), NEt<sub>4</sub>Br (>98%, Fluka), NH<sub>4</sub>Cl (>98%, Fluka), and LiBr (>98%, Fluka) were used as supplied.

**2.2. Absorption and Emission Spectra.** UV absorption spectra were recorded on a Perkin-Elmer Lambda 7 UV-vis absorption spectrometer. Steady-state fluorescence spectra were recorded on a Perkin-Elmer LS 50 Luminescence Spectrometer, and corrected for instrumental sensitivity. Time-resolved fluorescence measurements were performed on a single-photon-counting spectrometer. A nF 900 flashlight lamp (Edinburgh Instruments) was used for excitation, with a flash duration of 2–3 ns at 4 kV. The time resolution obtained with mono-exponential fluorescence decay was 2 ns. A specially designed software (Edinburgh Instruments), run on a personal computer, was used for data acquisition.

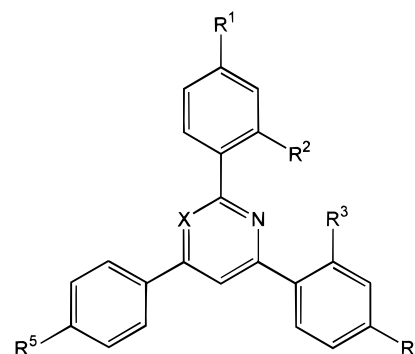
**2.3. NMR Spectra.** <sup>1</sup>H and <sup>13</sup>C NMR spectra were recorded on a Bruker ARX 500 NMR spectrometer, equipped with a 5-mm dual <sup>1</sup>H/<sup>13</sup>C probehead, at 500.13 and 125.76 MHz nominal frequency, respectively. Chemical shifts (δ) are given in ppm relative to tetramethylsilane (TMS) as internal standard.

**2.4. Cyclic Voltammetry.** Measurements were performed, under the control of the M 270 software, on a EG&G Princeton Applied Research potentiostat/galvanostat, with a three-electrode array of glassy carbon working electrode, platinum counter

## CHART 1: Structures and Designations

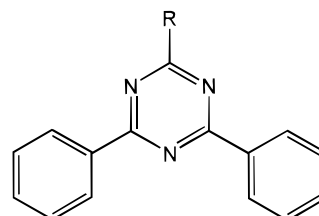


	R <sup>1</sup>	R <sup>2</sup>	R <sup>3</sup>	R <sup>4</sup>	R <sup>5</sup>	R <sup>6</sup>
M-MeO-P	OCH <sub>3</sub>	OCH <sub>3</sub>	H	H	H	H
D-MeO-P	OC <sub>12</sub> H <sub>25</sub>	OCH <sub>3</sub>	H	H	H	H
M-MeO-T	OCH <sub>3</sub>	OCH <sub>3</sub>	H	CH <sub>3</sub>	CH <sub>3</sub>	H
H-MeO-T	OC <sub>6</sub> H <sub>13</sub>	OCH <sub>3</sub>	H	CH <sub>3</sub>	CH <sub>3</sub>	H
M-MeO-X	OCH <sub>3</sub>	OCH <sub>3</sub>	CH <sub>3</sub>	CH <sub>3</sub>	CH <sub>3</sub>	CH <sub>3</sub>
D-MeO-X	OC <sub>12</sub> H <sub>25</sub>	OCH <sub>3</sub>	CH <sub>3</sub>	CH <sub>3</sub>	CH <sub>3</sub>	CH <sub>3</sub>
2-MOTT-2	H	OCH <sub>3</sub>	H	H	H	H
2-MOTT-4	OCH <sub>3</sub>	H	H	H	H	H
2,4-MOTT-4	OCH <sub>3</sub>	H	H	OCH <sub>3</sub>	H	H
2,4,6-MOTT-4	OCH <sub>3</sub>	H	H	OCH <sub>3</sub>	OCH <sub>3</sub>	H
2-HTT-2	H	OH	H	H	H	H
2,4-HTT-2	H	OH	OH	H	H	H
TPT	H	H	H	H	H	H



	X	R <sup>1</sup>	R <sup>2</sup>	R <sup>3</sup>	R <sup>4</sup>	R <sup>5</sup>
HMD	N	OC <sub>6</sub> H <sub>13</sub>	OH	OH	OC <sub>6</sub> H <sub>13</sub>	OCH <sub>3</sub>
HDD	N	OC <sub>6</sub> H <sub>13</sub>	OH	OC <sub>6</sub> H <sub>13</sub>	OC <sub>6</sub> H <sub>13</sub>	OCH <sub>3</sub>
BHD	N	R'	OH	OH	R'	H
HDP	CH	H	OH	H	H	H

"R' = OCH<sub>2</sub>CH(OH)CH<sub>2</sub>OC<sub>4</sub>H<sub>9</sub>



N2-DTZ R = pyrrolidino  
 N3-DTZ R = piperidino  
 N4-DTZ R = morpholino

electrode, and Ag/AgCl reference electrode. Ferrocene (redox potential 0.34 V vs the normal hydrogen electrode<sup>40</sup>) was used as internal reference. Triazine concentrations in anhydrous acetonitrile were in the range 10<sup>-4</sup>–10<sup>-5</sup> M. Bu<sub>4</sub>NPF<sub>6</sub> was used as conducting salt. Scan rates were between 100 mV/s and 40 000 mV/s.

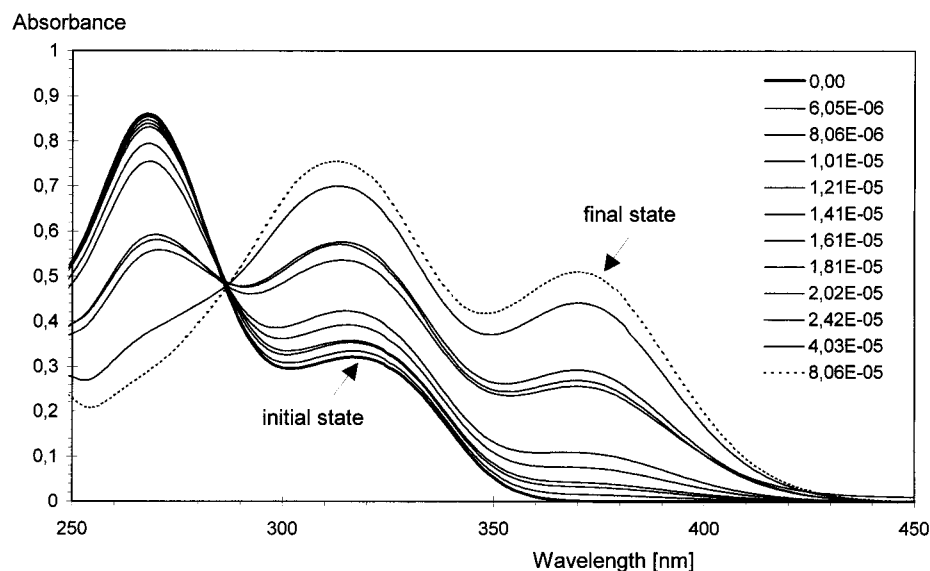


**Figure 1.** UV absorption spectra of M-MeO-P in acetonitrile with increasing proton concentration (adjusted by addition of  $10^{-5}$  M HClO<sub>4</sub>;  $0-8 \times 10^{-5}$  M).

**2.5. Photobleaching Apparatus.** The photostability of the individual triazines was tested with a mercury high-pressure lamp 500-W HBO. To remove unwanted IR and short-wavelength ( $\lambda < 300$  nm) UV radiation, the light was filtered through a cooled saturated copper sulfate solution, and then focused, via a system of lenses, onto the sample, enclosed in a thermostated cuvette and stirred to ensure homogeneous distribution during irradiation.

**2.6.  $pK_a$  Measurements.** Because of the poor solubility of the triazines in water,  $pK_a$  values were determined in acetic anhydride, by titration with 0.1 N perchloric acid in acetic acid. The electrode potential was monitored potentiometrically with a Schott pH-meter CG 817 T and a Schott pH combination electrode N 1042 A. In a plot of electrode potential vs volume of acid added, a curve with two points of inflection is obtained the first of which is the half-neutralization point (hnp) where protonated and nonprotonated triazines are present in equal concentration. According to Gyenes<sup>41</sup> and Streuli,<sup>42</sup> hnp electrode potentials are proportional to the  $pK_a$  values measured in water. By determining the hnp values in acetic anhydride for a number of bases with known  $pK_a$ , a calibration line is obtained which directly correlates the hnp values determined for the triazines in acetic anhydride with their  $pK_a$  values in water.<sup>43</sup>

### 3. Protonation Studies

**3.1. UV Absorption Spectra.** The (methoxyaryl) triazines, in their nonprotonated form, generally display two UV absorption bands which are assigned, respectively,  $\pi\pi^*$  and charge transfer (CT) character (Table 1). The CT band arises from an intramolecular charge transfer from the electron-rich methoxyaryl moiety into the electron-deficient triazine ring, and consequently is missing in the absorption spectrum of the parent compounds *s*-triazine<sup>44,45</sup> and 2,4,6-triphenyl-1,3,5-triazine ( $\lambda_1$  268 nm; cf. ref 38 and references cited there). With the introduction of additional *para*-alkoxy groups, that is, with enhanced electron donation into the triazine  $\pi$  system, the  $\pi\pi^*$  band is shifted to longer, and the CT band to shorter wavelengths, resulting in increasing overlap of the two absorptions. Thus, two bands still appear in the acetonitrile spectrum of 2-MOTT-4 (for structures, see Chart 1) whereas 2,4-MOTT-4 and 2,4,6-MOTT-4 show one merged absorption band only. An *ortho*-methoxy substituent, in contrast, causes a severe twist

**TABLE 1: UV Absorption Maxima ( $\lambda_1$ :  $\pi\pi^*$  Band;  $\lambda_2$ : CT Band) of 1,3,5-Triazines in Protonated and Nonprotonated Form (in CH<sub>3</sub>CN)**

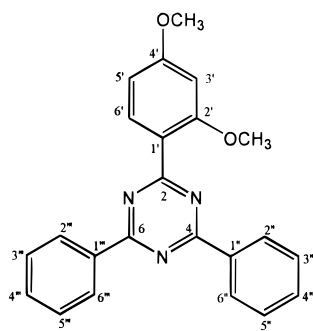
triazine	nonprotonated		protonated	
	$\lambda_1$ (nm)	$\lambda_2$ (nm)	$\lambda_1$ (nm)	$\lambda_2$ (nm)
M-MeO-P	267	313	313	370
D-MeO-P	267	318	310	369
M-MeO-T	280	316	337	367
H-MeO-T	280	319	337	371
M-MeO-X	277	320	340	366
D-MeO-X	278	318	340	371
2-MOTT-2	266	314	314	371
2-MOTT-4	271	298	368	—
2,4-MOTT-4		302		368
2,4,6-MOTT-4		304		375
N2-DTZ	260	—	267	—
N3-DTZ	260	—	267	—
N4-DTZ	260	—	267	—

between the methoxyaryl and the triazine ring, thus significantly reducing  $\pi\pi$  overlap and, concomitantly, charge transfer (cf. Table 1, 2-MOTT-2 vs 2-MOTT-4). The CT absorption displays distinct solvatochromy, and is shifted bathochromically with increasing solvent polarity.<sup>43</sup> The dialkylamino triazines N2-DTZ, N3-DTZ, and N4-DTZ where the electron-donating +M substituent is linked directly, and not through a phenyl moiety, to the triazine  $\pi$  system likewise lack the CT band.

Upon protonation, both the  $\pi\pi^*$  and the CT absorption maxima are shifted to the red relative to those of the nonprotonated compounds (Table 1). The clearly defined isosbestic points in the absorption spectra (shown for M-MeO-P in Figure 1) constitute unequivocal proof of an equilibrium between protonated and nonprotonated species in the ground state. For N2-DTZ, N3-DTZ, and N4-DTZ, the bathochromic protonation shift is remarkably small.

**3.2. Site of Protonation in 1,3,5-Triazines.** For a closer look at the regiochemistry of the protonation, <sup>1</sup>H and <sup>13</sup>C NMR spectra were recorded of both nonprotonated and protonated M-MeO-P. The triazine NMR data we have reported so far were generally obtained in CDCl<sub>3</sub>.<sup>38</sup> In protonated form, however, triaryl triazines are too sparingly soluble in CDCl<sub>3</sub>, especially for <sup>13</sup>C measurements; spectra for the present work were therefore taken in the dipolar solvent CD<sub>3</sub>CN. Between CDCl<sub>3</sub> and CD<sub>3</sub>CN, almost all carbon resonances experience a

**TABLE 2:**  $^1\text{H}$  and  $^{13}\text{C}$  Chemical Shifts [ $\delta$  (ppm)] for 2-(2,4-Dimethoxyphenyl)-4,6-diphenyl-1,3,5-triazine (M–MeO–P) in Nonprotonated and Protonated Form (in  $\text{CD}_3\text{CN}$  and  $\text{CD}_3\text{CN}/\text{H}_2\text{SO}_4$ , Respectively)



position	nonprotonated		protonated ( $\text{H}_2\text{SO}_4$ )	
	$\delta$ ( $^1\text{H}$ )	$\delta$ ( $^{13}\text{C}$ )	$\delta$ ( $^{13}\text{C}$ )	$\delta$ ( $^1\text{H}$ )
2		173.61	170.64	
4,6		172.03	170.64	
1'		119.68	108.46	
2' <sup>a</sup>		162.35	163.48	
3'	6.733	100.53	100.00	6.878
4' <sup>a</sup>		165.10	164.81	
5'	6.724	106.74	110.61	6.939
6'	8.273	134.84	135.89	8.861
2'-OCH <sub>3</sub> <sup>b</sup>	3.982	57.02	58.94	4.321
4'-OCH <sub>3</sub> <sup>b,c</sup>	3.908	56.42	57.49	4.031
1'',1'''		137.49	≈131'	
2'',6'',2''',6''' <sup>d,e</sup>	8.708	129.73	131.05	8.610
3'',5'',3''',5''' <sup>d,e</sup>	7.606	129.85	130.88	7.766
4'',4'''	7.656	133.55	137.41	7.901
$\text{CD}_3\text{CN}$	1.941	1.39		1.992
		118.38	118.43	

<sup>a</sup> Assignment of C-2'/C-4' may have to be interchanged. <sup>b</sup> In both protonated and nonprotonated form, the high- and low-field OCH<sub>3</sub> carbon resonances are correlated, respectively, with the high- and low-field proton signal. <sup>c</sup> For nonprotonated M–MeO–P, the 4'-OCH<sub>3</sub> carbon resonance is assigned by virtue of the identical chemical shift, in both  $\text{CDCl}_3$  and  $\text{CD}_3\text{CN}$ , with that of the three *para*-OCH<sub>3</sub> groups in 2,4,6-MOTT-4. <sup>d</sup>  $^{13}\text{C}$  assignment for the 4,6-phenyl moieties is confirmed unequivocally by a  $^1\text{H},^{13}\text{C}$  COSY spectrum. Thus, the inversion of the relative position of the *ortho*- and *meta*- $^{13}\text{C}$  resonances, and especially the extreme low-field shift of the *para*- $^{13}\text{C}$  signal for the protonated species, is established beyond any doubt. <sup>e</sup> The *ortho*-carbon signal appears severely broadened upon protonation, that of the *meta*-carbon atoms but slightly; still, *o/m/p* signals integrate correctly 2:2:1. <sup>f</sup> The signal of the *ipso*-carbon atoms is broadened almost beyond recognition.

distinct downfield shift of  $1.0 \pm 0.3$  ppm, whereas the corresponding  $^1\text{H}$  nuclei appear slightly better shielded in most cases. None of the relative shifts show any indication of a significantly modified electron distribution within the molecule, however. This changes dramatically upon protonation.

In Table 2,  $^1\text{H}$  and  $^{13}\text{C}$  chemical shifts are listed for M–MeO–P in  $\text{CD}_3\text{CN}$ , together with those for M–MeO–P, protonated with  $\text{H}_2\text{SO}_4$ , also in  $\text{CD}_3\text{CN}$  (0.8 mL, with 100–200  $\mu\text{L}$   $\text{H}_2\text{SO}_4$  added). The  $\text{C}_2$  symmetry of the parent structure appears conserved in the NMR spectra of the protonated form, M–MeO–P–H<sup>+</sup>: there is one common resonance only for C-4,6 (accidentally coinciding with the C-2 signal), and for all  $^1\text{H}$  and  $^{13}\text{C}$  nuclei in the respective positions of the two phenyl substituents at C-4,6. This could be caused by protonation of the triazine ring exclusively at N-5, that is, *para* to the dimethoxyaryl group. Fixed protonation at either N-1 or N-3 would result in a clear differentiation between the two positions C-4 and C-6, and thence of the two phenyl substituents. This distinction will be canceled out again, however, by a rapid

equilibrium between the three prototropic forms. The isobestic points, upon protonation, in the UV spectrum of M–MeO–P, as well as the results of NMR protonation studies for the symmetrical derivatives, 2,4,6-triphenyl- and 2,4,6-tris(4-methoxyphenyl)-1,3,5-triazine (TPT and 2,4,6-MOTT-4, respectively; see below) clearly show protonation to be in fact rapidly reversible on the NMR time scale ( $> 10^{2-3}/\text{s}$ ).

**3.3. Ground-State Charge Transfer in Protonated Triaryltriazines.** The *para* phenyl proton (4'',4'''–H) multiplet in M–MeO–P–H<sup>+</sup> is shifted *downfield*, relative to that of the nonprotonated form, by +0.25 ppm, the signal of the *para* carbon atom by + 3.85 ppm (see Table 2, Figure 2). The *ortho* proton multiplet, in contrast, has moved *upfield* by 0.1 ppm upon protonation. The triazine  $^{13}\text{C}$  resonances (C-2,4,6) likewise appear distinctly better shielded. Most striking, however, is the enormous upfield shift of –11 ppm for the *ipso* carbon C-1' in the resorcinyl moiety, and of – 6.5 ppm for the *ipso* carbon atoms C-1'',1''' in the two phenyl groups.

If one considers the triazine core, with respect to the three aryl rings, as an electron-withdrawing substituent, its –M character will be enhanced substantially in protonated form. An increased resonance effect should manifest itself comparably in the respective *ortho* and *para* positions. The *ortho* protons 2'',6'',2''',6'''–H are shifted *upfield*, however, in M–MeO–P–H<sup>+</sup>, and the downfield shift of the corresponding  $^{13}\text{C}$  resonances C-2'',6'',2''',6''' appears much attenuated relative to that of the *para* carbon atoms C-4'',4'''. The extreme high-field shift of C-1' and, to a lesser extent, of C-1'',1''' cannot be accommodated with this model.

The protonated triazine ring rather seems to constitute a localized positive charge, drawing the polarizable  $\pi$ -electron cloud of all three aryl substituents toward the heterocyclic core of the molecule, and thus depleting the *para* positions of electron density; at the same time, electron density will increase especially in the respective *ipso* position. This phenomenon directly parallels the enhanced charge transfer from aryl into triazine  $\pi$ -system observed in the electron spectra of the protonated form.

The electron spectra (cf. section 3.1) show a substantial twist between resorcinyl and triazine ring in M–MeO–P, due to the *ortho* methoxy group; the concomitant decrease in  $\pi,\pi$ -overlap will result in reduced mesomeric interaction between the  $\pi$ -donor and  $\pi$ -acceptor systems. This argument does not hold for an inductive effect upon the  $\pi$ -electron distribution within the aryl substituents. It is only reasonable, thus, that the effect manifests itself in all three aryl moieties of M–MeO–P–H<sup>+</sup>. Actually, the high-field shift for the *ipso* carbon resonance is twice as large for the resorcinyl as for the phenyl group; this simply mirrors the additional electron-donating potential of the two methoxy substituents.

Identical results are obtained for the corresponding parent triazines, 2,4,6-triphenyl- and 2,4,6-tris(4-methoxyphenyl)-1,3,5-triazine (TPT and 2,4,6-MOTT-4, respectively). In Table 3, the  $^1\text{H}$  and  $^{13}\text{C}$  NMR data for the nonprotonated and protonated forms are juxtaposed as for M–MeO–P in Table 2. The solvent resonances, included once more, demonstrate that the shifts, induced by the change in medium upon adding  $\text{H}_2\text{SO}_4$ , are more than 1 order of magnitude smaller than those observed for the triazines; these shifts thence must be intrinsically correlated with the change in electron distribution upon protonation.

Again, the  $\text{C}_3$  symmetry of the parent triazines seems to be conserved in the spectra of the protonated species, with one single signal for C-2,4,6 in the triazine ring. Also, *one set* only of  $^1\text{H}$  and  $^{13}\text{C}$  resonances is observed for the *three* aryl moieties

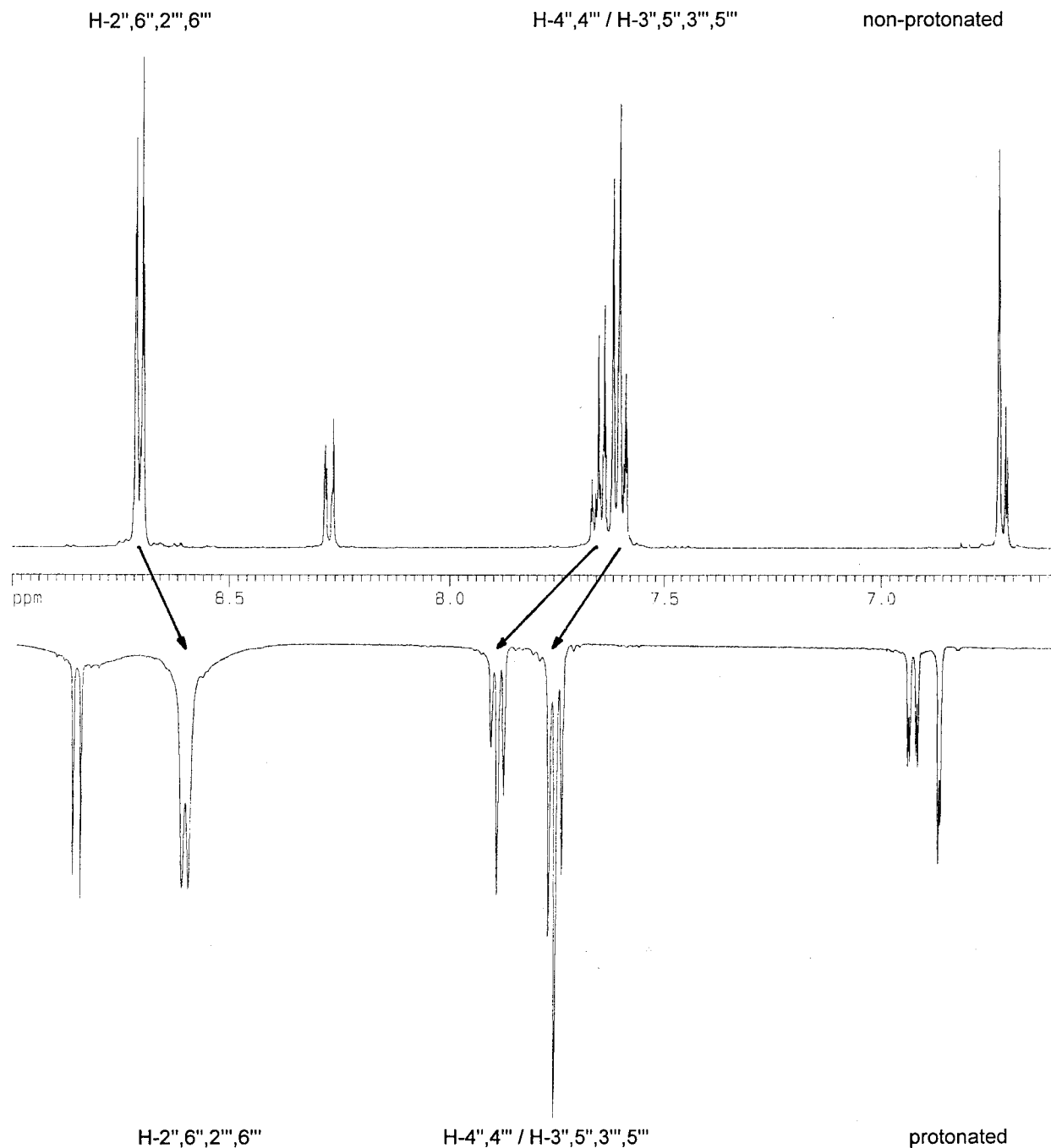


**Figure 2.** Partial  $^1\text{H}$  NMR spectrum (aryl proton region) of  $\text{M-MeO-P}$  in  $\text{CD}_3\text{CN}$  (upper trace) and protonated with concentrated  $\text{H}_2\text{SO}_4$  (inverted trace).

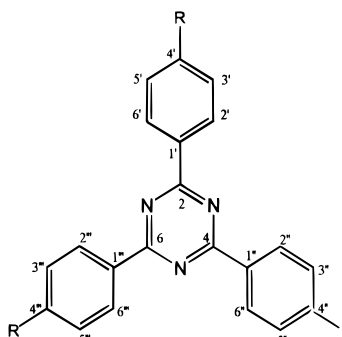
in both TPT and 2,4,6-MOTT-4. For this triazine, with a +M substituent in *para* position, the protonation shifts are somewhat attenuated relative to those for TPT, with the *ortho* protons shifted slightly less to higher, and the *meta* protons less to lower field. This clearly proves a substantial inductive polarization of the aryl substituent  $\pi$ -cloud by the triazine acceptor system already for the nonprotonated species. It is intriguing, by the way, that the high-field shift of the *ortho* and the low-field shift of the *meta* protons have identical values both in TPT ( $\pm 0.15$  ppm) and 2,4,6-MOTT-4 ( $\pm 0.12$  ppm; cf. Table 3).

**3.4. Photostability of 1,3,5-Triazines in Protonated and Nonprotonated Form.** All (methoxyaryl) triazines show severe changes in the UV absorption when tested for their light stability by 60–90 min of irradiation (shown for  $\text{M-MeO-P}$  in Figure 3; cf. Experimental Section). Photostability decreases in the

series  $\text{M/D-MeO-P} > \text{M/H-MeO-T} > \text{M/D-MeO-X}$ , that is, with an increasing number of methyl substituents in the 4-/6-aryl rings. The dialkylamino triazines N2-DTZ, N3-DTZ, and N4-DTZ are degraded photochemically in both protonated and nonprotonated form; however, the rate of degradation is lower in each case for the protonated species.

The triazines  $\text{M-}$  and  $\text{D-MeO-P}$ ,  $\text{M-}$  and  $\text{H-MeO-T}$ , and  $\text{M-}$  and  $\text{D-MeO-X}$ , in contrast, proved resistant to irradiation upon protonation. Even after 300 min, the absorption spectra displayed only minute changes (demonstrated for  $\text{M-MeO-P}$  in Figure 4). This is not caused by formation, by acid ether cleavage, of the respective (2-hydroxyaryl) triazines which would be intrinsically more photostable. When, after irradiation, the solutions of the protonated triazines were neutralized again with pyridine, UV absorption spectra were

**TABLE 3:**  $^1\text{H}$  and  $^{13}\text{C}$  Chemical Shifts [ $\delta$  (ppm)] for 2,4,6-Triphenyl-1,3,5-triazine (TPT) and 2,4,6-Tris(4-methoxyphenyl)-1,3,5-triazine (2,4,6-MOTT-4) in Nonprotonated and Protonated Form (in  $\text{CD}_3\text{CN}$  and  $\text{CD}_3\text{CN}/\text{H}_2\text{SO}_4$ , Respectively)



TPT            R = H

2,4,6-MOTT-4    R =  $\text{OCH}_3$

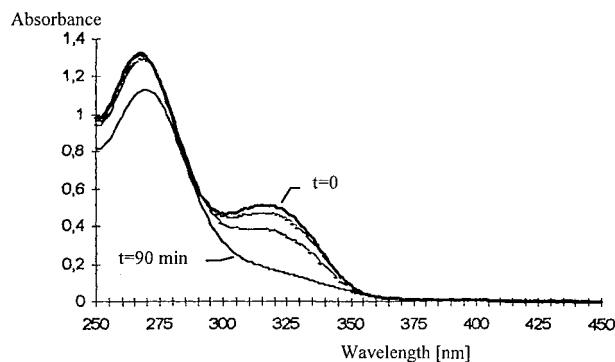
TPT position	nonprotonated		protonated ( $\text{H}_2\text{SO}_4$ )	
	$\delta$ ( $^1\text{H}$ )	$\delta$ ( $^{13}\text{C}$ )	$\delta$ ( $^{13}\text{C}$ )	$\delta$ ( $^1\text{H}$ )
2,4,6		172.69	169.89	
1',1'',1'''		137.16	130.92	
2'',6'',2''',6''',2''''',6'''''	8.804	129.96	132.06 <sup>a</sup>	8.657
3',5',3''',5''',3''''',5'''''	7.646	129.82	130.82 <sup>a</sup>	7.799
4',4'',4'''	7.697	133.89	137.81 <sup>a</sup>	7.952
$\text{CD}_3\text{CN}$	1.941	1.39 <sub>6</sub>	1.38 <sub>9</sub>	1.949
		118.39 <sub>2</sub>	118.40 <sub>0</sub>	

2,4,6-MOTT-4 position	nonprotonated		protonated ( $\text{H}_2\text{SO}_4$ )	
	$\delta$ ( $^1\text{H}$ )	$\delta$ ( $^{13}\text{C}$ )	$\delta$ ( $^{13}\text{C}$ )	$\delta$ ( $^1\text{H}$ )
2,4,6		171.75	167.74	
1',1'',1'''		129.79	? <sup>b</sup>	
2'',6'',2''',6''',2''''',6'''''	8.717	131.65	134.30	8.594
3',5',3''',5''',3''''',5'''''	7.133	115.15	116.25	7.251
4',4'',4'''		164.53	167.74	
4',4'',4'''- $\text{OCH}_3$	3.918	56.36	57.03	3.990
$\text{CD}_3\text{CN}$	1.941	1.39 <sub>6</sub>	1.38 <sub>6</sub>	1.946
		118.39 <sub>0</sub>	118.39 <sub>0</sub>	

<sup>a</sup> Assignments are unequivocally confirmed by  $^1\text{H},^{13}\text{C}$  COSY.

<sup>b</sup> Signal probably buried under the huge acetonitrile  $\text{C}\equiv\text{N}$  resonance.



**Figure 3.** Change in the UV absorption of M-MeO-P (in acetonitrile,  $c = 10^{-5}$  mol/L) upon irradiation with a HBO (high-pressure mercury) lamp ( $\lambda > 300$  nm) with traces run at  $t = 0, 30, 60, 90$  min.

obtained identical with those of the starting (methoxyaryl) triazines. The observed increase in photostability thence is intrinsically due to the protonated form.

**3.5.  $pK_a$  Values of 1,3,5-Triazines.** *Ground-State  $pK_a$  Values.* In Table 4,  $pK_a$  values (measured in acetic anhydride) are listed for methoxyaryl and hydroxyaryl triazines, together with those of some pyridine and pyrimidine derivatives (cf. Chart 1). As expected, the  $pK_a$  values decrease significantly in the order pyridine  $\rightarrow$  pyrimidine  $\rightarrow$  triazine derivatives: HDP 5.3; BHD, HDD, HMD 0.9–3.8; *s*-triazines  $-1.7$  to  $+2.3$ . The  $pK_a$  values of the various methoxyaryl triazines are all in the 0–2.3 range.

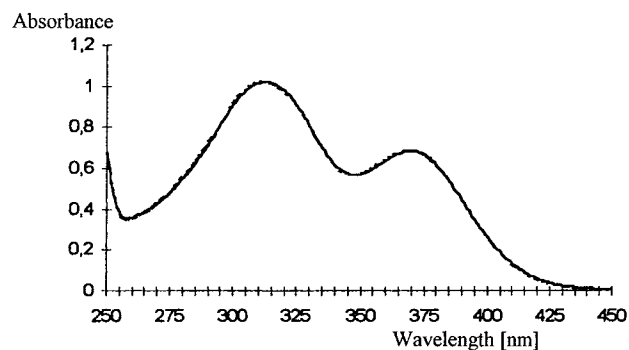


**Figure 4.** UV absorption of protonated M-MeO-P ( $c = 10^{-5}$  mol/L in acetonitrile,  $10^{-4}$  M  $\text{H}_2\text{SO}_4$ ) upon irradiation with a HBO lamp ( $\lambda > 300$  nm) after 0 and 90 min.

**TABLE 4:**  $pK_a$  Values for Pyridine, Pyrimidine, and 1,3,5-Triazine Derivatives, Determined in Acetic Anhydride

class of triazines	compound designation	$pK_a$
pyridines	HDP	5.3
	BHD	0.9
pyrimidines	HDD	2.0
	HMD	3.8
	1,3,5-triazines	
	2-HTT-2	-1.7
	2,4-HTT-2	-1.8
	N2-DTZ	3.6
	N3-DTZ	3.7
	N4-DTZ	3.6
	M-MeO-P	2.3
	M-MeO-T	0.5
	M-MeO-X	0.0
	2-MOTT-4	2.1
	2,4-MOTT-4	2.1
	2,4,6-MOTT-4	1.8
	2-MOTT-2	1.3

Only the dialkylamino triazines, with very strong electron donor substituents linked directly to the heterocyclic core, exhibit higher  $pK_a$  values (3.6–3.7). The decrease in basicity within the series pyridine  $\rightarrow$  pyrimidine  $\rightarrow$  triazine derivatives is a well-established phenomenon.<sup>46–49</sup> Competing electron acceptors in the heterocyclic core reduce the electron density at a given nitrogen atom; the basicity of nitrogen heterocycles consequently is lowered with each new aza center. The energy difference between polar resonance hybrids for the nonprotonated heterocycle and the (likewise polar) protonated species also increases with each aza nitrogen introduced in *meta* position.

*Excited-State  $pK_a$  Values.* The change in electron distribution upon photoexcitation often causes a drastic alteration in the acidity/basicity of a molecule. We therefore recorded fluorescence spectra at various pH values. Because acetic anhydride itself is strongly fluorescent, these measurements had to be performed in acetonitrile. The  $pK_a^*$  values therefore could not be determined directly, on the basis of the Förster Cycle (Scheme 1; cf. refs 50–52), because the ground-state  $pK_a$  values in Table 4 are all referenced to water (cf. Experimental Section, 2.6). The differences in  $pK_a$  between excited and ground state are sufficient for the subsequent discussion, however.

Fluorescence maxima and quantum yields are listed in Table 5 for several triazines in both protonated and nonprotonated form. With the exception of M- and D-MeO-P, there is a well-defined isostilbic point in the fluorescence spectra at various pH values upon excitation at the wavelength of the respective isosbestic point (shown for 2,4-MOTT-4 in Figure 5; cf. also section 4.2). Because the acid concentration ( $\sim 10^{-5}$  M) is too small for establishing the new protolytic equilibrium

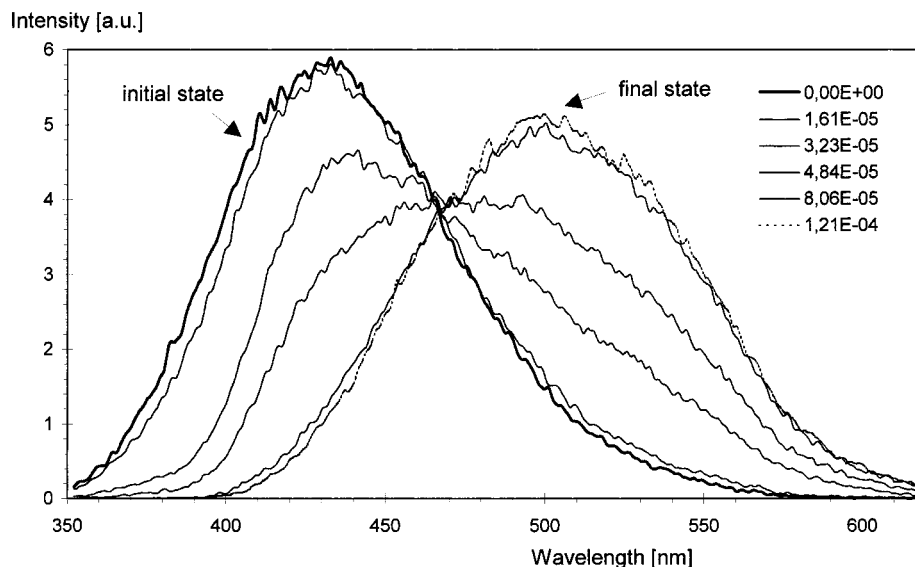


Figure 5. Fluorescence spectra of 2,4-MOTT-4 in acetonitrile ( $\lambda_{\text{exc}}$  313 nm) with increasing proton concentration ( $10^{-5}$  M HClO<sub>4</sub>).

**SCHEME 1: Förster Cycle – Relative Position of the Singlet States of the Acid BH<sup>+</sup> and Its Conjugate Base B (with  $E_1$  and  $E_2$  as the Respective 0.0 Transition Energies, and  $D, D^*$  the Respective Enthalpies of Dissociation for the Acid in the Ground and Excited State)**

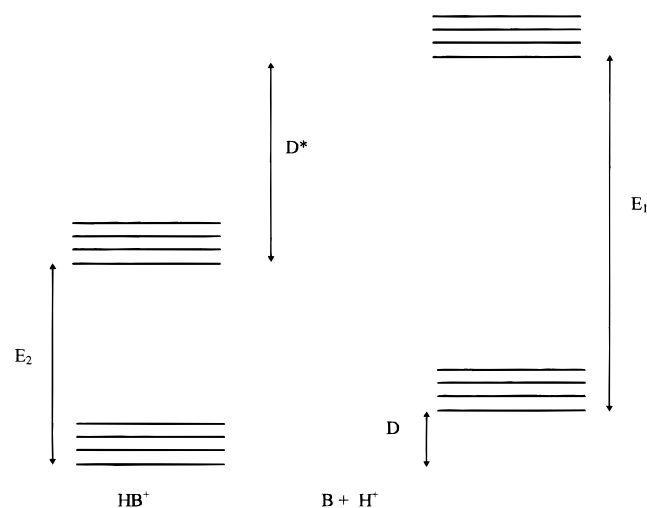


TABLE 5: Fluorescence Maxima and Quantum Yields for the Triazines in Acetonitrile

triazine	nonprotonated		protonated	
	$\lambda_{\text{max}}$ (nm)	$\Phi_{\text{F}} \cdot 10^3$	$\lambda_{\text{max}}$ (nm)	$\Phi_{\text{F}} \cdot 10^3$
M–MeO–P	460	18.5	—	—
D–MeO–P	460	24.9	—	—
M–MeO–T	452	10.0	519	0.3
H–MeO–T	451	14.0	518	0.5
M–MeO–X	432	1.3	511	0.7
D–MeO–X	421	2.3	519	0.7
2-MOTT-4	444	13.1	482	7.2
2,4-MOTT-4	437	19.9	501	3.95
2,4,6-MOTT-4	414	10.8	489	3.10
2-MOTT-2	422	1.3	530	0.18

between the excited protonated and nonprotonated forms during their short lifetime (2–3 ns), the observed fluorescence mirrors the molar ratio of the two forms in the ground state. Absence of a prototropic equilibrium in the excited state has already been demonstrated for an anthryl dimethyl aniline.<sup>53</sup>

TABLE 6: 0.0 Transition Wavelengths and Energies ( $E_1$  and  $E_2$ , Respectively) and Stokes' Shifts for the Triazines in Nonprotonated and Protonated Form (in Acetonitrile), and  $\Delta E_{0,0}$  ( $= E_1 - E_2$ ) and  $\Delta \text{p}K_{\text{a}}$  ( $= \text{p}K_{\text{a}}^* - \text{p}K_{\text{a}}$ ) Values Calculated Therefrom

triazine	nonprotonated			protonated			$\Delta \text{p}K_{\text{a}}$
	$\lambda_{00}$ (nm)	$E_1$ (kJ/mol)	Stokes' shift (cm <sup>-1</sup> )	$\lambda_{00}$ (nm)	$E_2$ (kJ/mol)	$\Delta E_{0,0} = E_1 - E_2$ (kJ/mol)	
M–MeO–P	369	324.2	10210	—	—	—	—
D–MeO–P	369	324.2	9707	—	—	—	—
M–MeO–T	356	336.0	9521	401	298.3	37.7	6.6
H–MeO–T	353	338.9	9175	400	299.1	39.8	7.0
M–MeO–X	348	343.7	7994	405	295.4	48.3	8.5
D–MeO–X	354	337.9	7693	409	292.5	45.5	8
2-MOTT-4	358	334.2	11035	404	296.1	38.1	6.7
2,4-MOTT-4	347	344.7	14017	407	293.1	50.8	8.9
2,4,6-MOTT-4	344	347.7	8740	396	302.1	45.6	8
2-MOTT-2	354	337.9	8150	400	299.1	38.8	6.8

In each case, absorption and emission of the protonated species are shifted to longer wavelengths relative to that of the nonprotonated triazine, that is,  $E_1$  is larger than  $E_2$ , and the energy of dissociation is higher in the excited than in the ground state ( $D^* > D$ , see Scheme 1). A comparative analysis of the fluorescence and absorption spectra of the nonprotonated and the corresponding protonated form affords the energy difference  $\Delta E_{0,0}$  between the 0.0 transitions of both species. The  $\Delta E_{0,0}$  values are rather large (38–51 kJ/mol, see Table 6), and correspond to  $\text{p}K_{\text{a}}$  differences of up to 9 units upon excitation if one neglects any difference in entropy between ground and excited state as proposed by Förster.<sup>50</sup> This behavior is typical for aza-nitrogen containing heterocycles,<sup>52,54–67</sup> and may be rationalized by mesomeric structures where the nitrogen atoms bear a negative charge being favored in the excited state. The concomitant increase of basicity in the excited relative to the ground state was verified experimentally first by Grabowska et al. for quinoxaline.<sup>68</sup>

#### 4. Energetic Stabilization by TICT States

We have previously reported<sup>38</sup> on the fluorescence kinetics of (nonprotonated) methoxyaryl triazines, and unequivocally established the existence of two different species in the excited state. The short-lived form ( $\tau_1 \approx 1.5$  ns) was identified with

the Franck–Condon (FC) state, the longer-lived species ( $\tau_2 \approx 4$  ns) was correlated with a TICT<sup>69</sup> state. For the mesityl derivative H–MeO–Ms, the two emitting species could even be spectrally separated.<sup>16</sup> The change of the fluorescence spectra with solvent viscosity and polarity indicates that, apart from a change in the dipole moment, a molecular reorientation takes place in the excited state which is best explained by the population of such TICT states. If it is not an FC but a TICT emission from the nonprotonated form that is detected,  $E_1$  (see Scheme 1) must be lower than the energy of both the principally excited FC state and the 0.0 transition. In this case, the intercept of absorption and fluorescence spectrum for the nonprotonated species no longer corresponds to the 0.0 transition.<sup>68</sup> The degree of stabilization by TICT differs between individual triazines. For nonprotonated amines, Tsutsumi et al.<sup>70</sup> have established a linear correlation between Stokes shift and  $pK_a^*$  value.

**4.1. Contribution of Protonated TICT States.** The entries in Table 6 show that the  $\Delta pK_a$  ( $= pK_a^* - pK_a$ ) values vary rather widely within a series of triazines. This can be interpreted as a consequence of energetic stabilization by a TICT state. If  $\Delta pK_a$  is plotted vs the Stokes' shift  $\Delta\tilde{\nu}$  ( $= \Delta\tilde{\nu}_{\text{abs}} - \Delta\tilde{\nu}_{\text{fluo}}$ ) for the nonprotonated triazines, and the correlation extrapolated to  $\Delta\tilde{\nu} = 0$ , the intercept with the ordinate relates to a non-solvent-stabilized FC state.<sup>43</sup> The value of 6.4, obtained for  $(\Delta pK_a)_{\Delta\tilde{\nu}=0} = (\Delta pK_a)_{\text{FC}}$ , is close to the experimental  $\Delta pK_a$  value of 6.8 for 2-MOTT-2 (cf. Table 6); this compound experiences a much smaller change in dipole moment upon excitation than all other triazines investigated here. The Stokes shift for 2-MOTT-2 likewise is very small and indicates that the excited state of the nonprotonated form of 2-MOTT-2 has scarcely any TICT character, and therefore appears energetically very close to a pure FC state.

The  $\Delta pK_a$  values for the (methoxyaryl) triazines, collected in Table 6, span a range between 6.6 and 8.9. The difference between the mean value  $(\Delta pK_a)_{\text{av}} = 7.55$  and  $(\Delta pK_a)_{\text{FC}}$  is 1.15, and may serve as a measure for the mean energetic stabilization of the TICT relative to the FC state. An energy difference of  $-6.5$  kJ/mol between these two excited states is calculated from eq 1 (in this case in acetonitrile).

$$\Delta\Delta E_{\text{FC} \rightarrow \text{TICT}} = RT \ln 10 [(\Delta pK_a)_{\text{FC}} - (\Delta pK_a)_{\text{av}}] \quad (1)$$

The energy of the TICT state can be expressed quantitatively in terms of the donor ionization potential IP(D), the electron affinity of the acceptor EA(A), the Coulomb energy  $E_C$ , and the solvation energy  $E_{\text{solv}}$  by eq 2.

$$E_{\text{TICT}} = \text{IP(D)} - \text{EA(A)} - E_C - E_{\text{solv}} \quad (2)$$

For the protonated species, the enhanced electron affinity of the acceptor lowers the energy of the TICT level<sup>69</sup>; the energy difference between ground and excited state of the protonated triazine thus is reduced. This becomes immediately apparent from the large  $(E_1 - E_2)$  values (see Table 6). In accordance with the well-known energy-gap law,<sup>71</sup> radiationless deactivation thence is accelerated for the protonated triazines, and the fluorescence quantum yield concomitantly reduced (cf. Table 5 and section 3.5).

**4.2. Proton-Induced Quenching of Fluorescence.** For M– and D–MeO–P, this proton-induced fluorescence quenching is particularly dramatic; no fluorescence at all is observed for the protonated form of these derivatives. When the fluorescence intensity of M–MeO–P is plotted vs the acid concentration (in acetonitrile), according to the Stern–Volmer equation<sup>72</sup> (eq 3, Figure 6), a Stern–Volmer constant  $K_q = 4.6 \times 10^4$  L/mol

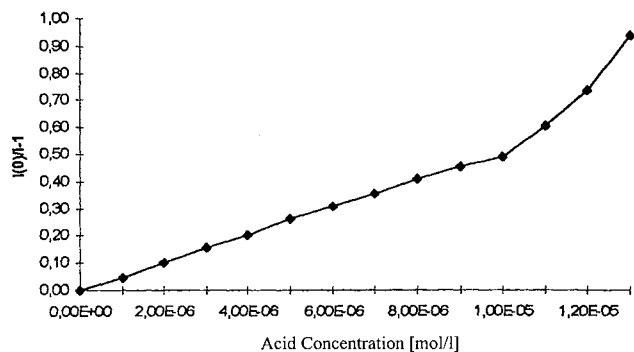


**Figure 6.** Stern–Volmer plot of emission intensities ( $\lambda_{\text{exc}}$  287 nm,  $\lambda_{\text{obs}}$  460 nm) for M–MeO–P vs acid concentration (varied by addition of 0.1 N HClO<sub>4</sub> in acetic acid).

is obtained from the experimental quenching data.

$$\frac{I_0}{I} - 1 = K_q C_{\text{H}^+} \quad (3)$$

where  $I_0/I$  = fluorescence intensity without/in the presence of acid;  $K_q$  = Stern–Volmer constant;  $C_{\text{H}^+} \approx C_{\text{HClO}_4}$ .

From the change in the absorption spectrum upon HClO<sub>4</sub> addition (cf. Figure 1), a  $pK_a$  value of 4.7 is determined for M–MeO–P in acetonitrile (the  $pK_a$  value for M–MeO–P in Table 3 refers to acetic anhydride as solvent). The Stern–Volmer constant for pure static quenching of M–MeO–P may also be calculated according to eq 4.

$$\frac{I_0}{I} = \frac{C_0}{C_B} = \frac{C_0(C_{\text{H}^+} + K_a)}{C_0 \cdot K_a} = 1 + \frac{C_{\text{H}^+}}{K_a} \quad (4)$$

with

$$C_B = \frac{C_0 \cdot K_a}{C_{\text{H}^+} + K_a} \quad \text{and} \quad C_0 = C_B + C_{\text{BH}^+}$$

where  $C_B/C_{\text{BH}^+}$  = concentration of non-protonated/protonated form of the triazine.

Equation 5, obtained by combining eqs 3 and 4, is valid under the assumption that only the nonprotonated molecule B fluoresces at the wavelength considered, and that an equilibrium is established between protonated and nonprotonated form in the ground state.

$$K_q (\text{static}) = K_a^{-1} = 10^{4.7} = 5 \times 10^4 \text{ L/mol} \quad (5)$$

This calculated  $K_q$  value is in good agreement with the constant  $K_q$  determined from the Stern–Volmer plot (cf. Figure 6 and above).

Analogous results were obtained for D–MeO–P. It can be inferred thence that a static quenching process is responsible for the proton-induced fluorescence quenching of all the (methoxyaryl) triazines considered here. At acid concentrations  $\geq 10^{-5}$  M, the correlation line in Figure 6 shows a distinct inflection in slope which very likely indicates at least a partial change to a more efficient quenching mechanism. For straight-forward dynamic, that is, diffusion-controlled quenching ( $\tau_F \approx 3$  ns), however, the acid concentration is not sufficiently high. At the moment, this problem is addressed by further studies.

It has been demonstrated unequivocally, however, that the photostability of the protonated triazines is increased dramatically by rapid radiationless deactivation. As already mentioned, protonated M– and D–MeO–P display no fluorescence at all; with the other triazines, what fluorescence is observed is



**TABLE 7: Fluorescence Quenching of (Methoxyaryl) Triazines in Acetonitrile upon Addition of Alkali and Tetraalkylammonium Halides<sup>a</sup>**

$\tau_f$ (ns)	$\Delta\mu$ (D)	$E_{red}$ (V)	quencher ( $E_{ox}$ ) triazine	$K_q \cdot 10^{-9}$ (L mol <sup>-1</sup> )/ $k_q \cdot 10^{-9}$ [L mol <sup>-1</sup> s <sup>-1</sup> ]						
				KI (1.4 V)	NaI (1.4 V)	NEt <sub>4</sub> I (1.4 V)	KSCN (1.5 V)	NEt <sub>4</sub> Br (1.9 V)	NHex <sub>4</sub> Cl (2.35 V)	LiBr (2.0 V)
—	15.8	-1.78	2-MOTT-4	15.91/—	13.29/—	14.57/—	9.15/—	12.62/—	4.22/—	3.72/—
3.07	12.9	-1.73	2,4-MOTT-4	14.66/4.78	12.25/3.99	7.03/2.29	8.35/2.72	7.85/2.56	<0.2/—	4.11/1.34
—	2.4	-1.91	2,4,6-MOTT-4	5.22/—	9.8/—	4.72/—	1.91/—	1.77/—	<0.2/—	0.87/—
—	-3.2	-1.78	2-MOTT-2	3.62/—	3.01/—	1.66/—	0.42/—	<0.2/—	<0.2/—	<0.2/—
3.35	17.1	-1.79	M-MeO-P	31.42/9.38	28.86/8.61	32.64/9.74	19.34/5.77	14.29/4.27	14.74/4.40	7.11/2.12
1.54	15.0	-1.88	M-MeO-T	17.00/11.0	17.67/11.5	14.73/9.56	7.95/5.16	8.66/5.62	6.07/3.94	1.23/0.80
1.41	9.8	-1.98	M-MeO-X	6.73/4.77	1.58/1.12	<0.2/—	0.50/0.35	<0.2/—	<0.2/—	<0.2/—

<sup>a</sup> Fluorescence lifetime,  $\tau_f$ ; changes in dipole moment upon photoexcitation,  $\Delta\mu = \mu_e - \mu_g$  (values for M-MeO-P, M-MeO-T, M-MeO-X from ref 38, for the other compounds from ref 73); Stern-Volmer constants,  $K_q$ ; quenching rate constants,  $k_q$ ; reduction potentials,  $E_{red}$ , for the triazines vs NHE<sup>40</sup> (determined by cyclic voltammetry); and oxidation potentials of the quencher salts,  $E_{ox}$  (quencher), vs SCE.<sup>76</sup>

significantly weaker than for the respective nonprotonated species.

### 5. Photochemical Stabilization by Intermolecular Electron Transfer

We have also investigated the influence of various salts with electron-donating anions on the fluorescence quantum yield of several triazines. Cyclic voltammetry<sup>74,75</sup> in acetonitrile (cf. Experimental Section) has established that the highly negative reduction potential of the triazines (between -1.73 and -1.98 V, cf. Table 7) forestalls any reduction in the ground state. Only upon UV excitation, sufficient energy is available for this process.

The reduction potential becomes more negative in the series M-MeO-P → M-MeO-T → M-MeO-X; this reflects the +I effect of the additional methyl substituents in the respective 4,6-aryl functions. If one assumes equal 0.0 transition energies for these triazines, the inference seems obvious that the electron-transfer rate is diminished in the same order; in fact, this was confirmed by our measurements.

Cyclic voltammetry has demonstrated that all (methoxyaryl) triazines undergo reversible one-electron transfer (shown for M-MeO-P in Figure 7). The free enthalpy for the electron transfer  $\Delta G_{ET}$  may be calculated from the reduction potential  $E_{red}(A/A^-)$ , measured for the acceptor, the 0.0 transition energy  $E_{0,0}$ , and the oxidation potential of the donor  $E_{ox}(D^-/D)$ .<sup>75-79</sup>

$$\Delta G_{ET} = nFE_{ox}(D^-/D) - nFE_{red}(A/A^-) - E_{0,0} - \frac{(Z^+Z^-)Fe^2}{4\pi\epsilon_0\epsilon_r a} \quad (6)$$

where  $n$  = number of electrons transferred;  $F$  = Faraday constant;  $a$  = encounter distance;  $Z^+/Z^-$  = number of electronic charges of, respectively, electron donor/acceptor;  $\epsilon_0/\epsilon_r$  = permittivity of vacuum/solvent.

Because the electron acceptor is not charged ( $Z^+ = 0$ ), the Coulomb term in eq 6 is zero for the systems considered here, that is, no Coulomb interaction is possible between both molecules either before or after electron transfer. The rate constant for this electron-transfer  $k_{ET}$  is assumed to equal the quenching rate constant  $k_q$  which is calculated from the Stern-Volmer constant  $K_q$  and the fluorescence lifetime  $\tau_f$  as  $k_q = K_q/\tau_f$ .

The UV absorption spectrum of the triazines appears unchanged upon addition of electron-donating salts. If there was any fluorescence quenching, it would thence have to be limited to the excited state. The corresponding dynamic quenching process is described quantitatively by the Stern-Volmer equa-

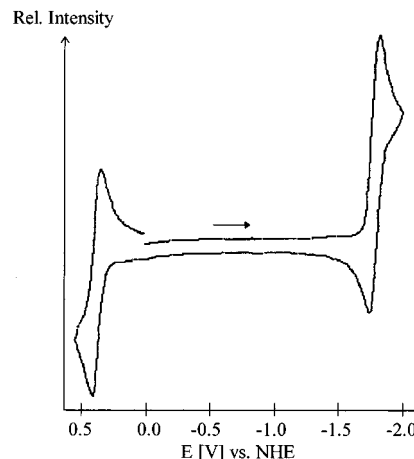


**Figure 7.** Cyclic voltammogram for M-MeO-P in CH<sub>3</sub>CN (right-hand wave; 0.1 M Bu<sub>4</sub>NPF<sub>6</sub>, 100 mV/s scan speed) and of the reference ferrocene (left-hand wave).

tion (equivalent to eq 3). Table 7 presents the results of quenching experiments with a series of alkali and tetraalkylammonium halides in acetonitrile. The Stern-Volmer constant  $K_q$  decreases in the series M-MeO-P > M-MeO-T > M-MeO-X (cf. Table 7), in line with the gradation of the dipole moment changes  $\Delta\mu$  upon photoexcitation. Because the ground-state dipole moments of these triazines do not differ significantly,<sup>38</sup> charge separation must be greater for the excited state of M-MeO-P than for that of M-MeO-T and M-MeO-X. The same relation between  $K_q$  and  $\Delta\mu$  is observed in the series 2-, 2,4-, 2,4,6-MOTT-4 where both parameters decline simultaneously.

With  $10^9$ – $10^{10}$  L mol<sup>-1</sup> s<sup>-1</sup>, the quenching rate constants  $k_q$  are in the order of rate constants for diffusion-controlled reactions (see Table 7). The rather long fluorescence lifetime observed for M-MeO-P ( $\tau_f = 3.35$  ns) accounts for the comparatively large  $K_q$  ( $= \tau_f \times k_q$ ) value of this compound. There is a distinct change of dipole moments upon excitation (Table 7) as well as a pronounced bathochromic shift of the fluorescence maximum of nonprotonated M-MeO-P (cf. Tables 1 and 5). These experimental results indicate that the excited molecule is quenched in a TICT state. A Rehm-Weller plot<sup>78,79</sup> of  $\log k_q$  vs  $\Delta G_{ET}$  (calculated from eq 6) shows that all electron-transfer rates lie in the range of diffusion control; this is plausible considering that most of the  $\Delta G_{ET}$  values are negative. Because of the fast transformation rate  $k_T$ , the TICT state is formed from the short-lived FC state despite the presence of quenching molecules. Thus, for kinetic reasons, only the long-lived TICT state can be quenched at the quencher concentrations used.

The very efficient quenching of fluorescence by anions ( $I^-$ ,  $Br^-$ ,  $SCN^-$ , see Table 7) will enhance the photostability of all the (methoxyaryl) triazines investigated here. Because, as shown, only dynamic quenching is possible with the electron-transfer mechanism, the effect is less pronounced than in protonation.

## 6. Conclusion

If one considers these results from a practical point of view, deactivation by electron transfer processes appears to be of more practical relevance than protonation. This would require addition of acids to UV stabilizing systems which does not seem very desirable. Addition of electron donors such as nontoxic inorganic salts, on the other hand, should present no practical problems. Electron transfer proved less efficient in our experiments, however, than protonation which has a stabilizing effect on the protonated (methoxyaryl) triazines in the ground state. Electron transfer, in contrast, is possible only in the excited state, due to the low reduction potential of the triazines.

## References and Notes

- Heller, H. J. *Eur. Polym. J. Suppl.* **1969**, 105–132.
- Heller, H. J.; Blattmann, H. R. *Pure Appl. Chem.* **1972**, *30*, 145–165; **1974**, *36*, 141–161.
- Werner, T.; Kramer, H. E. A.; Kuester, B.; Herlinger, H. *Angew. Makromol. Chem.* **1976**, *54*, 15–29.
- Werner, T.; Woessner, G.; Kramer, H. E. A. *Photodegradation and Photostabilization of Coatings*; Pappas, S. P., Winslow, F. H., Eds.; ACS Symposium Series 151; American Chemical Society: Washington, DC, 1981; pp 1–18.
- Woessner, G.; Goeller, G.; Kollat, P.; Stezowski, J. J.; Hauser, M.; Klein, U. K. A.; Kramer, H. E. A. *J. Phys. Chem.* **1984**, *88*, 5544–5550.
- Woessner, G.; Goeller, G.; Rieker, J.; Hoier, H.; Stezowski, J. J.; Daltrozzo, E.; Neureiter, M.; Kramer, H. E. A. *J. Phys. Chem.* **1985**, *89*, 3629–3636.
- Goeller, G.; Rieker, J.; Maier, A.; Stezowski, J. J.; Daltrozzo, E.; Neureiter, M.; Port, H.; Wiechmann, M.; Kramer, H. E. A. *J. Phys. Chem.* **1988**, *92*, 1452–1458.
- Kramer, H. E. A. *Farbe + Lack* **1986**, *92*, 919–924.
- Kramer, H. E. A. In *Photochromism – Molecules and Systems*; Dürr, H., Bouas-Laurent, H., Eds.; Elsevier: Amsterdam, 1990; pp 654–684.
- Kieninger, M.; Scherf, H.; Stueber, G. J.; Fischer, P.; Schmidt, A.; Kramer, H. E. A. *Book of Abstracts*, 34th International IUPAC Symposium on Macromolecules, Prague, July 13–18, 1992; Contribution No. 8-P4.
- Rieker, J.; Lemmert-Schmitt, E.; Goeller, G.; Roessler, M.; Stueber, G. J.; Schettler, H.; Kramer, H. E. A.; Stezowski, J. J.; Hoier, H.; Henkel, S.; Schmidt, A.; Port, H.; Wiechmann, M.; Rody, J.; Rytz, G.; Slongo, M.; Birbaum, J. L. *J. Phys. Chem.* **1992**, *96*, 10225–10234.
- Kramer, H. E. A. In *13th International Conference on Advances in the Stabilization and Degradation of Polymers*; Lucerne, Switzerland, May 22–24, 1991; Book of Abstracts, Patsis, A. V., Ed.; The Institute of Material Science, State University of New York at New Paltz, 1991; pp 59–78.
- Kramer, H. E. A. *GIT Fachz. Lab.* **1996**, *40*, 1220–1222.
- Keck, J.; Kramer, H. E. A.; Port, H.; Hirsch, T.; Fischer, P.; Rytz, G. *J. Phys. Chem.* **1996**, *100*, 14468–14475.
- Keck, J.; Stueber, G. J.; Kramer, H. E. A. (a) In *19th International Conference on Advances in the Stabilization and Degradation of Polymers*; Lucerne, Switzerland, May 9–11, 1997; Book of Abstracts, Patsis, A. V., Ed.; The Institute of Material Science, State University of New York at New Paltz, 1997; pp 131–150. (b) *Angew. Makromol. Chem.* **1997**, *252*, 119–138.
- Keck, J.; Roessler, M.; Schroeder, C.; Stueber, G. J.; Waiblinger, F.; Stein, M.; LeGourrière, D.; Kramer, H. E. A.; Hoier, H.; Henkel, S.; Fischer, P.; Port, H.; Hirsch, T.; Rytz, G.; Hayoz, P. *J. Phys. Chem.* **1998**, *102*, 6975–6985.
- Rabek, J. F. In *Photostabilization of Polymers. Principles and Applications*, Elsevier Applied Science Publishers: London, 1990.
- Padron, A. J. C. *J. Photochem. Photobiol. A* **1989**, *49*, 1–39.
- Ghigino, K. P.; Scully, A. D.; Bigger, S. W. In *The Effects of Radiation on High Technology Polymers*; Reichmanis, E., O'Donnell, J. H., Eds.; ACS Symposium Series No. 381; American Chemical Society: Washington, DC, 1988; pp 57–79.
- Otterstedt, J.-E. A. *J. Chem. Phys.* **1973**, *58*, 5716–5725.
- Klöpffer, W. *Adv. Photochem.* **1977**, *10*, 311–358.
- Flom, S. R.; Barbara, P. F. *Chem. Phys. Lett.* **1983**, *94*, 488–493.
- Barbara, P. F.; Rentzepis, P. M.; Brus, L. E. *J. Am. Chem. Soc.* **1980**, *102*, 2786–2791, 5631–5635.
- Barbara, P. F., Trommsdorf, H. P., Eds. Special Issue on Proton Transfer. *Chem. Phys.* **1989**, *136*, 153–360.
- Arnaut, L. G.; Formosino, S. J. *J. Photochem. Photobiol. A* **1993**, *75*, 1–20.
- Formosino, S. J.; Arnaut, L. G. *J. Photochem. Photobiol. A* **1993**, *75*, 21–48.
- Ormson, S. M.; Brown, R. G. *Prog. React. Kinet.* **1994**, *19*, 45–91.
- LeGourrière, D.; Ormson, S. M.; Brown, R. G. *Prog. React. Kinet.* **1994**, *19*, 211–275.
- Wiechmann, M.; Port, H.; Laermer, F.; Frey, W.; Elsaesser, T. *Chem. Phys. Lett.* **1990**, *165*, 28–34.
- Wiechmann, M.; Port, H.; Frey, W.; Laermer, F.; Elsaesser, T. *J. Phys. Chem.* **1991**, *95*, 1918–1923.
- Wiechmann, M.; Port, H. *J. Lumin. Chem.* **1991**, *48/49*, 217–223.
- O'Connor, D. B.; Scott, G. W.; Coulter, D. R.; Gupta, A.; Webb, S. P.; Yeh, S. W.; Clark, J. H. *Chem. Phys. Lett.* **1985**, *121*, 417–422.
- Huston, A. L.; Scott, G. W. *J. Phys. Chem.* **1987**, *91*, 1408–1413.
- Catalán, J.; De Paz, J. L. G.; Torres, M. R.; Tornero, J. D. *J. Chem. Soc., Faraday Trans.* **1997**, *93*, 1691–1696.
- Catalán, J.; Perez, P.; Fabero, F.; Wilshire, J. F. K.; Claramunt, R. M.; Elguero, J. *J. Am. Chem. Soc.* **1992**, *114*, 964–966.
- Catalán, J.; Del Valle, J. C.; Fabero, F.; Garcia, N. A. *Photochem. Photobiol.* **1995**, *61*, 118–123.
- McGarry, P. F.; Jokusch, St.; Fujiwara, Y.; Kaprinidis, N. A.; Turro, N. J. *J. Phys. Chem. A* **1997**, *101*, 764–767.
- Stueber, G. J.; Kieninger, M.; Schettler, H.; Busch, W.; Goeller, B.; Franke, J.; Kramer, H. E. A.; Hoier, H.; Henkel, S.; Fischer, P.; Port, H.; Hirsch, T.; Rytz, G.; Birbaum, J.-L. *J. Phys. Chem.* **1995**, *99*, 10097–10109.
- Waiblinger, F.; Keck, J.; Stein, M.; Fluegge, A. P.; Kramer, H. E. A.; Leppard, D. *J. Phys. Chem. A* **2000**, *104*, 1100–1106.
- Kolthoff, F. G. T. *J. Phys. Chem.* **1965**, *69*, 311–358.
- Gyenes, I. In *Titration in nichtwässrigen Medien*; Ferdinand Enke Verlag: Stuttgart, 1970.
- Streuli, C. A. *Anal. Chem.* **1958**, *30*, 997–1000.
- Elbe, F. Ph.D. Thesis; Universität Stuttgart, 1997.
- Hirt, R. C.; Halverson, F.; Schmitt, R. G. *J. Chem. Phys.* **1954**, *22*, 1148–1149.
- Brinen, J. S.; Goodman, L. *J. Chem. Phys.* **1959**, *31*, 482–487; **1961**, *35*, 1219–1225.
- Albert, A.; Goldacre, R.; Phillips, J. *J. Chem. Soc.* **1948**, 2240–2249.
- Brown, D. J. In *The Pyrimidines*; Brown, D. J., Ed.; Interscience Publishers: New York, 1962; pp 477–498.
- Brown, D. J. *Chem. Heterocycl. Compd.* **1970**, *16-S1*, 1–1127.
- Albert, A. In *Synthetic Procedures in Nucleic Acid Chemistry*; Zorbach, W. W., Tipson, R. S., Eds.; J. Wiley & Sons: New York, 1973; Vol. 2, pp 1–123.
- Förster, Th. *Z. Elektrochemie* **1950**, *54*, 42–46.
- Weller, A. In *Progress of Reaction Kinetics*; Porter, G., Ed.; Pergamon: London, 1961; Vol I, pp 187–214.
- Mordzinski, A.; Grabowska, A. *Chem. Phys. Lett.* **1982**, *90*, 122–127.
- Shizuka, H.; Ogiwara, T.; Kimura, E. *J. Phys. Chem.* **1985**, *89*, 4302–4306.
- Weller, A. *Z. Elektrochem.* **1952**, *56*, 662–668.
- Marzzacco, C. J.; Decey, G.; Colarulli, R.; Siuzdak, G.; Halpern, A. M. *J. Phys. Chem.* **1989**, *93*, 2935–2939.
- Kubin, J.; Testa, A. C. *J. Photochem. Photobiol. A* **1994**, *83*, 91–96.
- Dhruzhinin, S. I.; Dmitruk, S. L.; Lyapustina, S. A.; Uzhinov, B. M.; Makarova, N. I.; Knyazhanskii, M. I. *J. Photochem. Photobiol. A* **1992**, *68*, 319–335.
- Tsutsumi, T.; Shizuka, H. *Chem. Phys. Lett.* **1977**, *52*, 485–488.
- Dey, J. K.; Dogra, S. K. *Chem. Phys.* **1990**, *143*, 97–107.
- Förster, Th. *Chem. Phys. Lett.* **1972**, *17*, 309–311.
- Shizuka, H.; Nihira, H.; Shinozaki, T. *Chem. Phys. Lett.* **1982**, *93*, 208–212.
- Kishi, T.; Tanaka, J.; Kouyama, T. *Chem. Phys. Lett.* **1976**, *41*, 497–499.
- Tobita, S.; Shizuka, H. *Chem. Phys. Lett.* **1980**, *75*, 140–144.
- Shizuka, H.; Ishii, Y.; Morita, T. *Chem. Phys. Lett.* **1977**, *51*, 40–44.
- Lee, J.; Robinson, G. W.; Bassez, M.-P. *J. Am. Chem. Soc.* **1986**, *108*, 7477–7480.

- (66) Stryer, L. *J. Am. Chem. Soc.* **1966**, *88*, 5708–5712.
- (67) Hafner, F.; Wörner, J.; Steiner, U.; Hauser, M. *Chem. Phys. Lett.* **1980**, *73*, 139–144.
- (68) Grabowski, Z. R.; Grabowska, A. *Z. Phys. Chem. N. F.* **1976**, *56*, 197–208.
- (69) Rettig, W. *Top. Curr. Chem.* **1994**, *169*, 253–299.
- (70) Tsutsumi, K.; Seikiguchi, S.; Shizuka, H. *J. Chem. Soc., Faraday Trans.* **1982**, *78*, 1087–1101.
- (71) Englmann, R.; Jortner, J. *Mol. Phys.* **1970**, *18*, 145–164.
- (72) Stern, O.; Volmer, M. *Physik. Z.* **1919**, *20*, 183.
- (73) Stueber, G. J. Ph.D. Thesis; Universität Stuttgart, 1994.
- (74) Wawzonek, S.; Laitinen, H. A. *J. Am. Chem. Soc.* **1942**, *64*, 2365–2368.
- (75) Laitinen, H. A.; Wawzonek, S. *J. Am. Chem. Soc.* **1942**, *64*, 1765–1768.
- (76) Watkins, A. R. *J. Phys. Chem.* **1974**, *78*, 2555–2558.
- (77) Shizuka, H.; Nakamura, M.; Morita, T. *J. Phys. Chem.* **1980**, *84*, 989–994.
- (78) Rehm, D.; Weller, A. *Ber. Bunsen-Ges. Phys. Chem.* **1969**, *73*, 843–839.
- (79) Rehm, D.; Weller, A. *Israel J. Chem.* **1970**, *8*, 259–271.